

Variable Thumb Moment Arm Modeling and Thumb-Tip Force Production of a Human-Like Robotic Hand

Taylor D. Niehues

Department of Mechanical Engineering,
The University of Texas at Austin,
Austin, TX 78712
e-mail: taylor.niehues@utexas.edu

Ashish D. Deshpande

Mem. ASME
Department of Mechanical Engineering,
The University of Texas at Austin,
Austin, TX 78712
e-mail: ashish@austin.utexas.edu

The anatomically correct testbed (ACT) hand mechanically simulates the musculoskeletal structure of the fingers and thumb of the human hand. In this work, we analyze the muscle moment arms (MAs) and thumb-tip force vectors in the ACT thumb in order to compare the ACT thumb's mechanical structure to the human thumb. Motion data are used to determine joint angle-dependent MA models, and thumb-tip three-dimensional (3D) force vectors are experimentally analyzed when forces are applied to individual muscles. Results are presented for both a nominal ACT thumb model designed to match human MAs and an adjusted model that more closely replicates human-like thumb-tip forces. The results confirm that the ACT thumb is capable of faithfully representing human musculoskeletal structure and muscle functionality. Using the ACT hand as a physical simulation platform allows us to gain a better understanding of the underlying biomechanical and neuromuscular properties of the human hand to ultimately inform the design and control of robotic and prosthetic hands. [DOI: 10.1115/1.4037402]

1 Introduction

The human thumb plays a key role in hand functionality, inspiring researchers to use several unique methodologies to uncover the thumb's underlying biomechanical and neuromuscular properties. Cadaveric studies have proven effective for determining the thumb's musculoskeletal structure and biomechanical properties [1,2], while in vivo experimentation [3–5] allows for observation of the coordinated muscle activation patterns that produce appropriate thumb motions and forces during everyday tasks. Biomechanical thumb modeling [6,7] is a valuable tool for interpreting the collected human data and providing a comprehensive understanding of how biomechanical structure and neuromuscular control each contribute to provide thumb functionality.

The anatomically correct testbed (ACT) hand is a robotic system that mechanically simulates the musculoskeletal structure of the fingers and thumb of the human hand. Our idea is to use this robotic system, which closely imitates human hand musculoskeletal structure, as a physical simulation platform for studying the underlying mechanisms behind human hand dexterity to ultimately inform the design of robotic and prosthetic hands. While it is understood that both musculoskeletal structure and neuromuscular control contribute to the amazing capabilities of the human hand, exactly how these elements interact is still not clear. The capabilities of current robotic and prosthetic hands are still limited when compared to human hand dexterity. The ACT hand opens up a number of research possibilities for gaining a fundamental understanding of hand functionality that may result in design guidelines for artificial hands. For example, implementation of accepted robotic hand control methodologies on the ACT hand's human-like tendon structure can provide unique insights into the benefits of the hand's mechanical structure and may simultaneously stimulate innovations in the field of robotic hand control. We can also develop and test novel control algorithms for the ACT hand motivated by observed human neuromuscular control paradigms, e.g., the sensory-dependent finger forces observed in human studies [4], with the goal of understanding how our brains

are able to utilize the hand's unique musculoskeletal structure to achieve amazing dexterity.

Designing a robotic thumb that captures the critical properties of the human thumb is a challenging task. Thus far, researchers have been unable to develop a biomechanical thumb model that accurately reproduces human data [8,9], most likely due to the thumb's mechanical complexity, high anatomic variability [10], and the inherent challenges of conducting in vivo and cadaveric experiments. Without the existence of a well-defined thumb model, we cannot make a definitive claim that the ACT thumb represents a valid human thumb model. In this work, we will present an iterative design process for the ACT thumb as we attempt to reproduce multiple sources of human thumb data from literature as closely as possible. Thus far, research with the ACT hand's index finger has revealed key insights into the biomechanical structure of the human index finger [11], while only preliminary testing has been performed on the ACT thumb [12,13].

In this work, we analyze the muscle moment arms (MAs) and thumb-tip force vectors in the ACT thumb in order to compare the ACT thumb's mechanical structure to the human thumb. The nominal ACT thumb tendon structure was designed to closely match cadaveric moment arm data reported by Smutz et al. [1]. Motion data were used to determine the joint-dependent ACT muscle moment arms. The ACT thumb's human-like muscle functionality was then analyzed by collecting three-dimensional (3D) thumb-tip force vectors produced when forces were applied to the ACT muscle/tendon units. An adjusted ACT thumb was designed with slightly altered tendon routing to improve the matching of ACT thumb-tip forces to human data reported by Pearlman et al. [2]. Results are presented for both ACT models, along with a sensitivity analysis to show how changes in tendon moment arms affect thumb-tip forces. We discuss choosing the ideal ACT model to best replicate the human thumb's mechanics depending on the desired task parameters, such as the expected magnitude of tendon forces.

2 Methods

The ACT thumb is designed with the five nonorthogonal, nonintersecting anatomical degrees-of-freedom [6,14,15], and eight musculotendon actuator units (see Fig. 1). Details for the ACT thumb

Manuscript received November 14, 2016; final manuscript received July 12, 2017; published online August 16, 2017. Assoc. Editor: Zong-Ming Li.

can be found in the work of Deshpande et al. [13]. While the internal joint structure is comprised of an aluminum beam structure, the bone shells, including tendon routing points, are manufactured using an SLA 3D printer (Form 1+, FormLabs Inc., Somerville, MA). Thus, the physical MAs of the system can be adjusted by modifying the CAD models and subsequent reprinting of the bone shells.

We begin by comparing the MAs of the ACT thumb with cadaveric thumb MA data reported in Ref. [1]. In their work, Smutz et al. [1] define the carpometacarpal (CMC) flexion/extension and abduction/adduction joint axes as orthogonal to the plane of the palm, which differs significantly from the anatomical CMC joint axes [14] in the ACT thumb [12]. Therefore, ACT CMC joint axes are defined with respect to two virtual CMC joint axes defined orthogonal to the palm for all subsequent MA analyses.

We individually recorded motion data for each joint using a motion capture system with active infrared light-emitting diode markers (PhaseSpace Inc., San Leandro, CA) while holding all other joints stationary. The motion capture system has been shown to be sufficiently accurate for finger pose estimation [16]. We perform additional validation tests to verify motion capture accuracy by placing multiple markers on a single bone segment and moving the thumb through its range of motion. The resulting marker distance estimations, which should remain constant, had a standard deviation of ± 0.8 mm and a maximum variation of 2 mm that occurred near joint limits where markers become more obscured. The maximum variation would result in a joint angle estimation error of ± 4 deg, which we deem to be acceptable for our study. Muscle excursion data were simultaneously recorded from encoders in the musculo-tendon actuator units with the tendons held taut by constant torsion springs. Data collection occurred at a rate of 480 Hz.

We trained three-layer feed-forward neural networks (NNs) [17] for each joint using the MATLAB Neural Network Toolbox (Mathworks Inc., Natick, MA) with joint angle (θ) as input and muscle lengths ($\ell \in \mathbb{R}^8$) as output to find forward kinematics

functions $\ell = \mathbf{f}_i(\theta_i)$ for each joint. Posture-dependent moment arm functions $\mathbf{R}_i(\theta_i)$ are found through differentiation

$$\mathbf{R}_i(\theta_i) = \frac{\partial \ell}{\partial \theta_i} = \frac{\partial \mathbf{f}_i(\theta_i)}{\partial \theta_i} \quad i = 1, \dots, 5 \quad (1)$$

In past work, other regression methods such as least-squares regression and Gaussian process regression (GPR) [11] have been used to learn $\mathbf{f}(\theta)$. We have chosen NNs because they have lower computational cost compared to GPR and do not require a user-defined parametric equation as does least-squares regression and many other smooth optimization techniques. The number of hidden nodes for each NN was chosen heuristically between 3 and 5 to match kinematic data without overfitting.

Next, we collected ACT thumb-tip force data for comparison with cadaveric data [2]. A multi-axis force/torque sensor (ATI Nano25, Apex, NC) was connected to the ACT thumb-tip while the thumb was statically positioned in either key or opposition pinch posture, and we manually applied muscle forces while also recording tendon tensions (Omega DFG55, Norwalk, CT). Thumb-tip force vectors are recorded while holding muscle tensions equal to the maximum muscle forces applied by Pearlman et al. [2].

In this work, we present the results from two distinct tendon routing designs. In the first case, the tendon origins, routing points, and insertions were specifically designed to match muscle MAs from cadaveric data [1]. However, as other researchers have also observed [9], a thumb model that matches reported MAs does not necessarily lead to matching of thumb-tip forces. Therefore, we also present the results from a second ACT tendon routing design with slight modifications, informed by a simulation model, to better match reported human thumb-tip forces.

Finally, the sensitivity of MA variations toward thumb-tip force matching was analyzed using a computer simulation thumb model. A nominal model based on human MA data leads to poor thumb-tip force matching, as already stated. Therefore, MAs and joint angles were optimized to generate a thumb model which accurately recreates thumb-tip force production of each muscle (see Table 2 for details of optimization). We then found the range of allowable variation for each MA while holding all others constant, with the requirement that corresponding thumb-tip force must remain within reported human ranges [2].

3 Results

Using forward kinematic NNs trained for each joint and Eq. (1), angle-dependent MA plots were generated for all five thumb joints (Figs. 2 and 3) and compared with cadaveric MA data reported by Smutz et al. [1]. The NN models were validated for separately collected test motion data, which showed a mean absolute error of less than 0.02 mm in all cases. We also cross-validated the MA curves generated using our NN method with MA curves generated using GPR with the same motion data in order to ensure the results are independent of the fitting method used. The MA plots are very similar for each case, with an average absolute error of 0.56 ± 0.51 mm for all muscle-joint combinations.

The nominal ACT model, designed to match human MAs, falls within experimental ranges in nearly all cases. Limitations preventing exact MA matching will be explored in more detail in Sec. 4. The adjusted model, designed to better match thumb-tip forces reported by Pearlman et al. [2], deviates from human MAs and in many cases falls outside of reported ranges.

We next compare the thumb-tip force vectors produced by each muscle to cadaveric data from Ref. [2]. The nominal model did not match the reported force vectors in the majority of cases in either opposition or key pinch postures, as seen in Table 1. However, in the adjusted model, tendon routing adjustments based on static thumb simulations lead to dramatically improved thumb-tip force matching, with nearly all thumb-tip forces falling within reported ranges (Fig. 4 and Table 1).

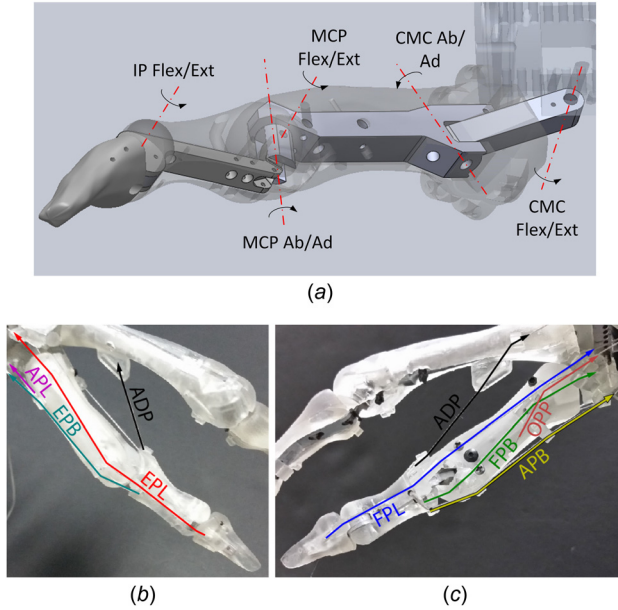


Fig. 1 Musculoskeletal structure of the ACT thumb. (a) The joint axes for the ACT thumb’s five anatomical degrees-of-freedom including flexion/extension and abduction/adduction of the CMC joint, flexion/extension and abduction/adduction of the metacarpophalangeal (MCP) joint, and flexion/extension of the interphalangeal (IP) joint. (b) Dorsal view of the ACT thumb showing the adductor pollicis longus (ADP), extensor pollicis longus (EPL), abductor pollicis longus (APL), extensor pollicis brevis (EPB) tendons. (c) Palmar view showing the flexor pollicis longus (FPL), flexor pollicis brevis (FPB), opponens (OPP), and abductor pollicis brevis (APB) tendons.

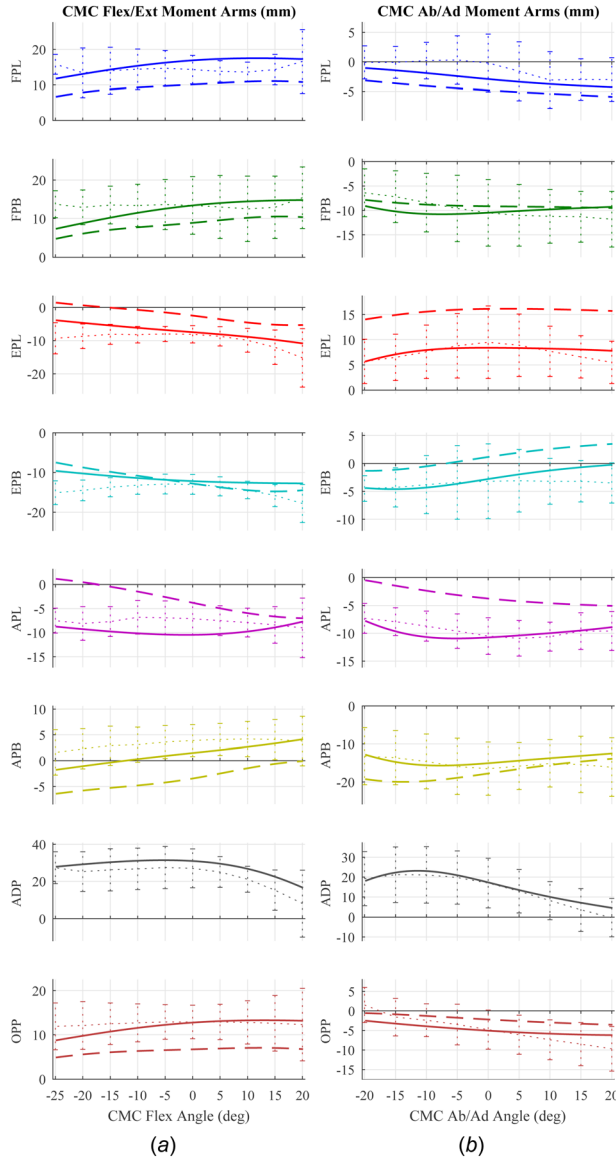


Fig. 2 ACT thumb MAs for (a) CMC flexion/extension and (b) CMC abduction/adduction (ab/ad) for the nominal model designed to match human MAs (solid lines) and the adjusted model designed to match thumb-tip forces (dashed lines, where modification was necessary), compared with experimental human data collected by Smutz et al. [1] (dotted lines with error bars, mean \pm 1SD). Positive angles and MAs for CMC ab/ad correspond to thumb adduction (toward the palm).

The MA sensitivity analysis indicates the necessary precision of each MA for thumb-tip force matching (Table 2). In general, flexion/extension MAs required higher precision than abduction/adduction MAs, likely due to the sensitivity of force magnitude and direction in the radial plane to the relative values of flexor MAs. Additionally, thumb-tip forces are much more sensitive to MA variations in opposition pinch as compared to key pinch. This is because the MCP joint is less flexed in opposition pinch (10 deg versus 45 deg), meaning the thumb is closer to a kinematic singularity position, near which small changes in joint torques result in large deviations in endtip force.

4 Discussion

Our results show that the ACT thumb is capable of faithfully representing human thumb mechanical structure and muscle

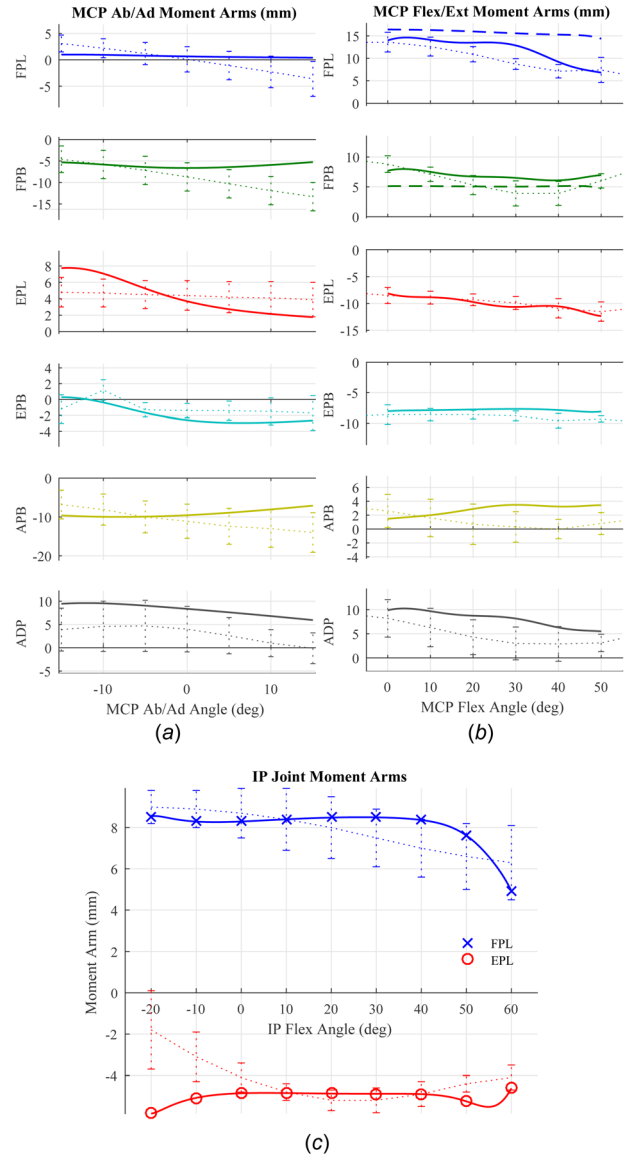


Fig. 3 ACT thumb MAs for (a) MCP abduction/adduction (ab/ad), (b) MCP flexion/extension, and (c) IP flexion/extension for the nominal model designed to match human MAs (solid lines) and the adjusted model designed to match thumb-tip forces (dashed lines, where modification was necessary), compared with experimental human data collected by Smutz et al. [1] (dotted lines with error bars, mean \pm 1SD). Positive angles and MAs for MCP ab/ad correspond to thumb adduction (toward the palm).

functionality. It has been noted in the literature that the MAs reported by Smutz et al. [1] should not be considered definitive [2,9]. Therefore, we first created a nominal ACT model based on MAs from Ref. [1]. Then, informed by our static computer simulation model and sensitivity analysis (Table 2), we determined the necessary modifications to ACT tendon routing to create an adjusted ACT model that better replicates thumb muscle functionality and thumb-tip force production as reported by Pearlman et al. [2].

The finding that a nominal biomechanical thumb model with experimental MAs reported by Smutz et al. [1] fails to replicate human-like thumb-tip force production has been reported in multiple previous works [8,9]. The level of variability present in the thumb's musculotendon routing [1] and joint structure [10] creates a normative model of a human thumb a challenging task. Additionally, there exist inconsistencies in the definitions of CMC joint axes, especially considering [1] defined CMC joint motions with

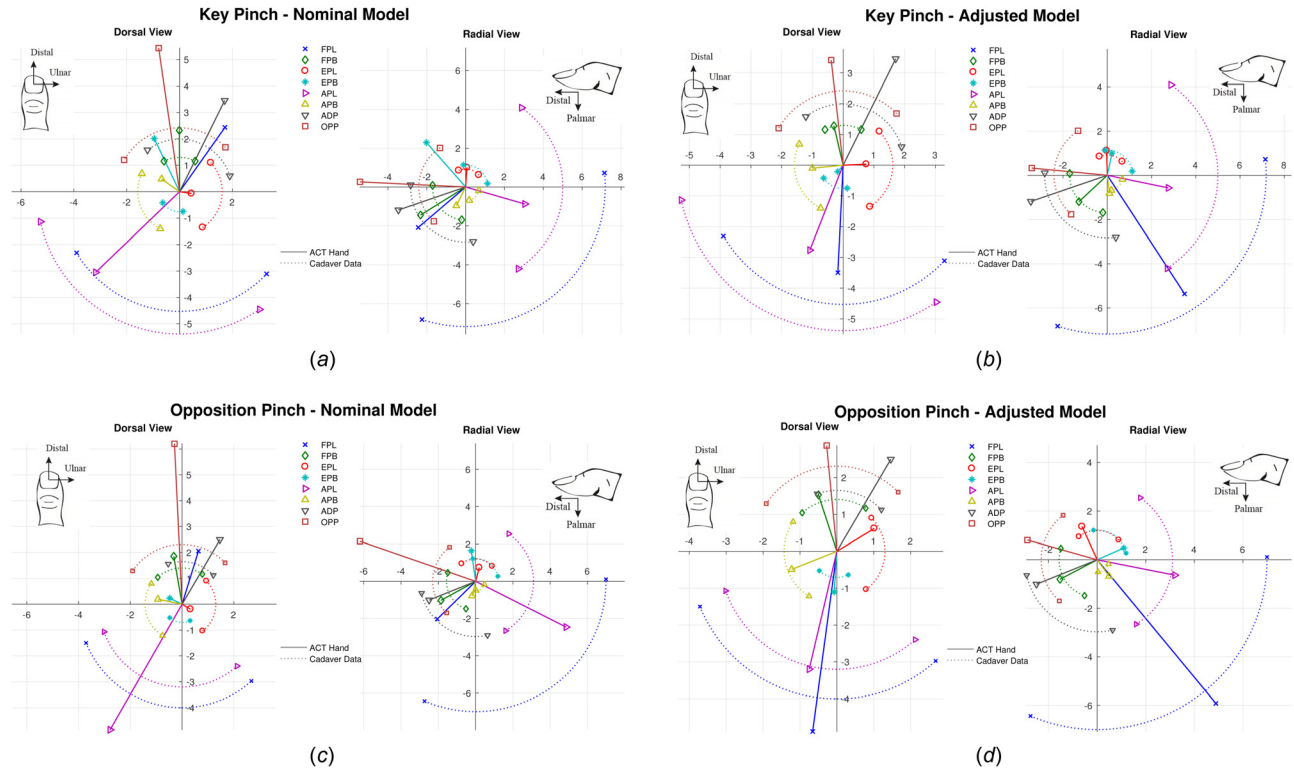


Fig. 4 Thumb-tip force data from the ACT thumb when forces are applied to each thumb muscle individually. All data are rotated to apply to a right hand. Muscle force values are identical to the maximum forces from cadaveric experiments in Ref. [2]. Results are shown for the nominal ACT thumb model, designed to match cadaveric MA measurements from Ref. [1], in (a) key pinch and (c) opposition pinch postures. For comparison, we show results from the adjusted model that was redesigned to better match thumb-tip forces from Ref. [2] in (b) key pinch and (d) opposition pinch postures. Solid lines represent experimental force vectors from the ACT thumb, and dashed arcs represent the magnitude (mean) and angle (mean \pm SD) of cadaveric data reported by Pearlman et al. [2]. The force vector is said to show a good directional match if it falls within the corresponding dashed arc. Actual values are reported in Table 1.

respect to the plane of the palm. Thus, a biomechanical thumb model using anatomical nonintersecting CMC joint axes from Ref. [14] requires CMC MA transformation, something that to our knowledge has not been addressed in the literature. Initial support of this claim is evidenced by superior force matching of the

nominal ACT model in Table 1, which accounts for the MA transformation, compared to the nominal simulation model in Table 2, which did not apply this transformation.

Analysis of the required modifications between the nominal and adjusted models can also provide insights into the sources

Table 1 Experimentally collected ACT thumb-tip force data

	FPL	FPB	EPL	EPB	APL	APB	ADP	OPP
<i>Opposition pinch</i>								
Nominal model								
$\ F\ _{\text{error}} (\%)^a$	57.8	34.0	51.3	43.6	90.9	17.9	2.1	185.7
$\phi_{\text{error}} (\text{deg})^b$	81.3	5.4	25.5	43.7	26.5	31.6	39.4	16.7
Adjusted model								
$\ F\ _{\text{error}} (\%)^a$	10.0	12.3	6.2	0.3	4.5	1.0	— ^c	30.2
$\phi_{\text{error}} (\text{deg})^b$	6.1	12.5	25.5	31.2	9.2	14.6	— ^c	13.2
<i>Key pinch</i>								
Nominal model								
$\ F\ _{\text{error}} (\%)^a$	49.5	60.8	42.0	166.5	15.3	25.1	50.8	129.2
$\phi_{\text{error}} (\text{deg})^b$	90.3	8.3	36.4	75.6	26.2	53.3	18.6	2.3
Adjusted model								
$\ F\ _{\text{error}} (\%)^a$	11.1	4.8	29.1	13.6	43.0	23.8	— ^c	43.9
$\phi_{\text{error}} (\text{deg})^b$	6.2	10.1	27.6	25.8	9.9	24.3	— ^c	0.9

^aForce magnitude error: $\|F\|_{\text{error}} = \frac{\|F_{\text{simulated}}\| - \|F_{\text{reported}}\|}{\|F_{\text{reported}}\|}$. Bold numbers indicate cases in which thumb-tip force magnitude is within experimental range (mean \pm SD) reported by Pearlman et al. [2].

^bForce direction error: $\phi_{\text{error}} = \cos^{-1} \left(\frac{F_{\text{simulated}} \cdot F_{\text{reported}}}{\|F_{\text{simulated}}\| \|F_{\text{reported}}\|} \right)$. Bold numbers indicate cases in which thumb-tip force directionality is within experimental ranges (mean \pm SD) reported by Pearlman et al. [2] in both the radial and dorsal planes (see Fig. 4).

^cModification of the ADP tendon was deemed to be unnecessary, because the thumb-tip force vector already matched human data well enough that it did not require adjustment (see Fig. 4). Thus, the ADP for nominal and adjusted models are identical.

Table 2 Sensitivity analysis of thumb-tip force production

	FPL	FPB	EPL	EPB	APL	APB	ADP	OPP
<i>Opposition pinch</i>								
Nominal model								
$\ F\ _{\text{error}} (\%)^a$	80.3	816.1	479.9	448.5	178.7	421.8	211.4	985.9
$\phi_{\text{error}} (\text{deg})^b$	10.0	98.9	56.5	63.5	44.7	66.0	79.5	42.6
Adjusted model ^c								
MA bounds	±1SD	±1SD	±1SD	±1.5SD	±1.5SD	±1SD	±1SD	±2SD
$\ F\ _{\text{error}} (\%)^a$	0.7	31.1	4.2	27.9	24.2	0.9	13.5	49.7
$\phi_{\text{error}} (\text{deg})^b$	2.8	4.9	0.0	2.3	39.8	0.0	4.3	32.7
Allowable variation (mm)								
CMC flex MA	1.2	1.6	1.3	1.3	0.9	1.8	2.8	3.6
CMC ab/ad MA	2.1	2.7	2.5	2.1	1.3	3.0	4.5	3.9
MCP ab/ad MA	0.9	1.1	0.9	0.9	—	1.4	2.0	—
MCP flex MA	0.5	0.7	0.5	0.6	—	0.8	1.1	—
IP flex MA	0.7	—	0.7	—	—	—	—	—
<i>Key pinch</i>								
Nominal model								
$\ F\ _{\text{error}} (\%)^a$	25.4	39.7	77.4	113.5	55.7	5.7	111.8	154.6
$\phi_{\text{error}} (\text{deg})^b$	141.3	22.9	62.6	63.1	32.8	76.0	48.7	29.4
Adjusted model ^c								
MA bounds	±2SD	±2SD	±1SD	±3SD	±1SD	±1SD	±1SD	±1SD
$\ F\ _{\text{error}} (\%)^a$	11.3	0.2	7.6	18.4	25.4	6.9	0.2	31.5
$\phi_{\text{error}} (\text{deg})^b$	9.3	0.0	21.0	5.7	19.4	12.4	0.0	16.7
Allowable variation (mm)								
CMC flex MA	3.6	8.1	7.0	4.4	6.5	6.6	10.5	8.2
CMC ab/ad MA	15.9	4.5	5.6	3.8	11.5	5.1	12.1	9.9
MCP ab/ad MA	12.6	4.6	5.4	3.4	—	3.4	10.4	—
MCP flex MA	1.2	4.2	2.6	2.3	—	2.3	5.8	—
IP flex MA	1.8	—	3.6	—	—	—	—	—

$$^a\text{Force magnitude error: } \|F\|_{\text{error}} = \frac{\|\mathbf{F}_{\text{simulated}}\| - \|\mathbf{F}_{\text{reported}}\|}{\|\mathbf{F}_{\text{reported}}\|}$$

$$^b\text{Force direction error: } \phi_{\text{error}} = \cos^{-1} \left(\frac{\mathbf{F}_{\text{simulated}} \cdot \mathbf{F}_{\text{reported}}}{\|\mathbf{F}_{\text{simulated}}\| \|\mathbf{F}_{\text{reported}}\|} \right)$$

^cAdjusted model obtained through minimization of the cost function $\|\mathbf{F}_{\text{simulated}} - \mathbf{F}_{\text{reported}}\|$, with MAs constrained to the indicated ranges from nominal values (SDs as reported by Smutz et al. [1]) to allow convergence of thumb-tip forces to within experimental ranges reported by Pearlman et al. [2]. For the APL and OPP (single-joint muscles), joint deviations of ± 15 deg were allowed at the MCP and IP flexion joints to facilitate directional fit, particularly in the radial plane [18].

of discrepancies between experimental human MAs [1] and experimental thumb-tip forces [2]. For example, in the nominal model, the monoarticular OPP and APL produced force magnitudes much larger than human thumb-tip data, so the adjusted model implemented reduced MAs for these two muscles. In the human thumb, it is possible that applying large tensions to the OPP or APL would lead to significant CMC joint translation due to inherent joint elasticity, which might similarly reduce their effective MAs.

The relationship between thumb-tip force and muscle tension in human thumbs has been reported to be nonlinear, most likely due to load-dependent bone translation and viscoelastic muscle-tendon paths [2]. The ACT thumb has an arrangement of rigid tendon routing points that are incapable of replicating force-dependent changes in tendon lines of action. Instead, researchers can use the tools developed here to, depending on the task parameters such as expected muscle forces, design custom tendon routing that can approximate the human thumb's muscle-to-endtip force transformation near the operating conditions they are exploring.

Although the ACT hand represents a powerful tool, there are inherent limitations that may affect the accuracy of these results. Differentiation of a fitted model has issues, especially near joint limits, which could affect the accuracy of presented MAs. Joint angles of the ACT thumb during thumb-tip force testing may not precisely match thumb postures in human studies, which could affect the resulting thumb-tip force vectors [18]. The joints in the ACT thumb are hinge joints, but bone translations and

sliding in human thumbs could result in a more complex kinematic model [19].

5 Conclusions

We have investigated the kinematic and force relationships of the ACT thumb and compared its mechanical structure to that of the human thumb. Motion data are used to determine joint angle-dependent MA models, and thumb-tip 3D force vectors are experimentally analyzed when forces are applied to individual muscles. Results are presented for both a nominal ACT thumb model designed to match human MAs and an adjusted model that more closely replicates human-like thumb-tip forces. We show that the ACT thumb is capable of replicating human thumb mechanical structure and muscle functionality, provided the tendon routing is properly adjusted to account for load-dependent moment arm changes near the operating muscle force conditions being investigated.

The results of this work open a number of avenues of research focused on the human thumb and hand. The ACT hand's electro-mechanical tendon actuation and software control system allow for experiments exploring how the hand's mechanical structure and neuromuscular control contribute to hand dexterity during dynamic interaction tasks. We plan to implement the key insights we gain through experimentation toward the design and control of robotic and prosthetic hands to ultimately achieve human-like performance.

Acknowledgment

The authors would like to thank Prashant Rao for his contributions toward the ACT hand project.

Funding Data

- National Science Foundation (Grant No. IIS-1157954).

References

- [1] Smutz, W. P., Kongsayreepong, A., Hughes, R. E., Niebur, G., Cooney, W. P., and An, K.-N., 1998, "Mechanical Advantage of the Thumb Muscles," *J. Biomech.*, **31**(6), pp. 565–570.
- [2] Pearlman, J. L., Roach, S. S., and Valero-Cuevas, F. J., 2004, "The Fundamental Thumb-Tip Force Vectors Produced by the Muscles of the Thumb," *J. Orthop. Res.*, **22**(2), pp. 306–312.
- [3] Johanson, M. E., Valero-Cuevas, F. J., and Hentz, V. R., 2001, "Activation Patterns of the Thumb Muscles During Stable and Unstable Pinch Tasks," *J. Hand Surg.*, **26**(4), pp. 698–705.
- [4] Nataraj, R., Audu, M. L., and Li, Z.-M., 2015, "Digit Mechanics in Relation to Endpoint Compliance During Precision Pinch," *J. Biomech.*, **48**(4), pp. 672–680.
- [5] Li, Z.-M., and Harkness, D. A., 2004, "Circumferential Force Production of the Thumb," *Med. Eng. Phys.*, **26**(8), pp. 663–670.
- [6] Giurintano, D., Hollister, A., Buford, W., Thompson, D., and Myers, L., 1995, "A Virtual Five-Link Model of the Thumb," *Med. Eng. Phys.*, **17**(4), pp. 297–303.
- [7] Holzbaur, K. R. S., Murray, W. M., and Delp, S. L., 2005, "A Model of the Upper Extremity for Simulating Musculoskeletal Surgery and Analyzing Neuromuscular Control," *Ann. Biomed. Eng.*, **33**(6), pp. 829–840.
- [8] Valero-Cuevas, F. J., Johanson, M. E., and Towles, J. D., 2003, "Towards a Realistic Biomechanical Model of the Thumb: The Choice of Kinematic Description May Be More Critical Than the Solution Method or the Variability/Uncertainty of Musculoskeletal Parameters," *J. Biomech.*, **36**(7), pp. 1019–1030.
- [9] Wohlman, S. J., and Murray, W. M., 2013, "Bridging the Gap Between Cadaveric and In Vivo Experiments: A Biomechanical Model Evaluating Thumb-Tip Endpoint Forces," *J. Biomech.*, **46**(5), pp. 1014–1020.
- [10] Santos, V. J., and Valero-Cuevas, F. J., 2003, "Anatomical Variability Naturally Leads to Multimodal of Denavit-Hartenberg Parameters for the Human Thumb," 25th Annual International Conference of the IEEE Engineering in Medicine and Biology Society (IEMBS), Cancun, Mexico, Sept. 17–21, Vol. 2, pp. 1823–1826.
- [11] Deshpande, A., Balasubramanian, R., Ko, J., and Matsuoka, Y., 2010, "Acquiring Variable Moment Arms for Index Finger Using a Robotic Testbed," *IEEE Trans. Biomed. Eng.*, **57**(8), pp. 2034–2044.
- [12] Chang, L., and Matsuoka, Y., 2006, "A Kinematic Thumb Model for the ACT Hand," IEEE International Conference on Robotics and Automation (ICRA), Orlando, FL, May 15–19, pp. 1000–1005.
- [13] Deshpande, A., Xu, Z., Weghe, M., Brown, B., Ko, J., Chang, L., Wilkinson, D., Bidic, S., and Matsuoka, Y., 2013, "Mechanisms of the Anatomically Correct Testbed Hand," *IEEE/ASME Trans. Mechatronics*, **18**(1), pp. 238–250.
- [14] Hollister, A., Buford, W. L., Myers, L. M., Giurintano, D. J., and Novick, A., 1992, "The Axes of Rotation of the Thumb Carpometacarpal Joint," *J. Orthop. Res.*, **10**(3), pp. 454–460.
- [15] Hollister, A., Giurintano, D. J., Buford, W. L., Myers, L. M., and Novick, A., 1995, "The Axes of Rotation of the Thumb Interphalangeal and Metacarpophalangeal Joints," *Clin. Orthop. Relat. Res.*, **320**, pp. 188–193.
- [16] Yun, Y., Agarwal, P., and Deshpande, A. D., 2015, "Accurate, Robust, and Real-Time Pose Estimation of Finger," *ASME J. Dyn. Syst. Meas. Control*, **137**(3), p. 034505.
- [17] McCulloch, W. S., and Pitts, W., 1943, "A Logical Calculus of the Ideas Immanent in Nervous Activity," *Bull. Math. Biophys.*, **5**(4), pp. 115–133.
- [18] Goehler, C. M., and Murray, W. M., 2010, "The Sensitivity of Endpoint Forces Produced by the Extrinsic Muscles of the Thumb to Posture," *J. Biomech.*, **43**(8), pp. 1553–1559.
- [19] Towles, J. D., Hentz, V. R., and Murray, W. M., 2008, "Use of Intrinsic Thumb Muscles May Help to Improve Lateral Pinch Function Restored by Tendon Transfer," *Clin. Biomech.*, **23**(4), pp. 387–394.